ELSEVIER

Journal of South American Earth Sciences 22 (2006) 239–254

Journal of
South American
Earth Sciences

www.elsevier.com/locate/jsames

Applying sandstone petrofacies to unravel the Upper Carboniferous evolution of the Paganzo Basin, northwest Argentina

Laura I. Net *, Carlos O. Limarino

CONICET – Departamento de Ciencias Geológicas, Universidad de Buenos Aires, Pabellón 2, Ciudad Universitaria, C1428EHA Buenos Aires, Argentina

Abstract

A compositional study of sandstones belonging to the lower section of the Paganzo Group (Middle Carboniferous–Early Permian) in the Paganzo Basin (northwestern Argentina) helps unravel the stratigraphic and paleogeographic evolution of the basin. Three morphotectonic units constitute the complex basement of the basin: (1) to the east, the igneous–metamorphic basement of the Sierras Pampeanas and Famatina systems; (2) to the west, the Precordillera, made up of Early and Middle Paleozoic sedimentary rocks; and (3) the Upper Paleozoic volcanic arc along the western boundary with the Río Blanco Basin. On the basis of sandstone detrital modes of the Lagares, Malanzán, Loma Larga, Guandacol, Tupe, Punta del Agua, and Río del Peñón formations, seven petrofacies are distinguished: quartzofeldespathic (QF), quartzofeldespathic-metamorphic enriched (QF-Lm), quartzofeldespathic-sedimentary enriched (QF-Ls), mixed quartzolithic (QL), quartzolithic-volcanic (QLv), volcanolithic-quartzose (LvQ), and volcanolithic (Lv). The spatial and temporal distribution of these petrofacies suggest an evolutive model for the Upper Paleozoic sedimentary filling of the basin that includes three "petrosomes": (1) the basement petrosome, a clastic wedge of arkosic composition that diachronically prograded and thinned from east to west; (2) the recycled orogen petrosome, revealing the Protoprecordillera as a positive element in the western Paganzo Basin during the Namurian; and (3) the volcanic arc petrosome, recording volcanic activity along the western margin of Gondwana during the Westphalian.

Keywords: Paganzo Basin; Carboniferous; Provenance; Petrofacies; Petrosomes

1. Introduction

Sandstone composition can be a powerful tool to analyze the evolution of sedimentary basins by revealing temporal and/or spatial variations in the participation of different source areas (e.g., Dickinson and Rich, 1972; Ingersoll, 1983; Ingersoll and Cavazza, 1991; Critelli and Ingersoll, 1995). Thus, detrital modes become an important source of information about regional changes in the nature of supply areas and paleogeographic modifications frequently linked to tectonic or magmatic activity. Although detrital modes of sandstones depend on not only the nature of the source area but also factors such as depositional environment, transport mechanism, climate, and diagenesis (e.g., Basu, 1986; Grantham and Velbel, 1988; Johnsson, 1993; Scasso and Limarino, 1997), useful information can be obtained if the impact of these factors is either limited (i.e., diagenesis still allows recognition of precursor grains) or can be constrained with additional geologic information (e.g., available paleoclimatic or paleogeographic reconstructions).

The Upper Paleozoic Paganzo Basin (Azcuy and Morelli, 1970a), located in northwest Argentina (Fig. 1), constitutes an excellent example to study the evolution of a complex basin by means of the analysis of the temporal and spatial variations of sandstone detrital modes. First, this basin exhibits a rich tectonic, magmatic, and climatic history that has been synthesized in several stratigraphic models (Limarino et al., 1988; LópezGamundı et al., 1989; González Bonorino, 1991; Fernández Seveso and

* Corresponding author. Present address: Apache Energía Argentina, S.R.L., Della Paolera 265 piso 24, C1001ADA Buenos Aires, Argentina. Tel.: +54 11 4320 9263; fax: +54 11 4314 2310.

E-mail addresses: laura.net@apachecorp.com (L.I. Net), limar@gl.fcen.uba.ar (C.O. Limarino).

0895-9811/$ - see front matter © 2006 Elsevier Ltd. All rights reserved.
doi:10.1016/j.jsames.2006.09.010

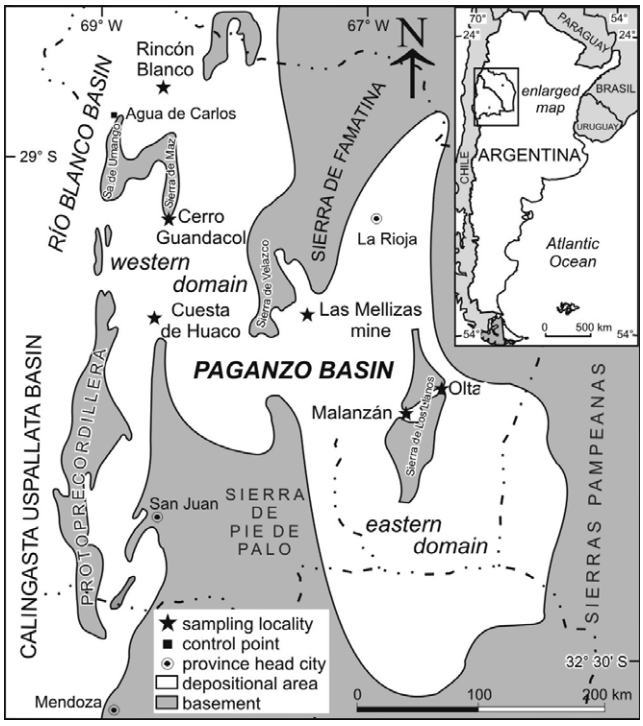

Fig. 1. Location map of Paganzo Basin in northwestern Argentina. Main morphostructural elements that constitute its basement and sampling localities are also shown.

Tankard, 1995). Second, previous diagenetic studies (e.g., Di Paola, 1972; Net, 1999) constrain the effect of postdepositional modifications for reconstructing the original sandstone composition.

Thus, a detailed compositional study of the sandstones of the lower section of the Paganzo Group (Bodenbender, 1896; Azcuy and Morelli, 1970b) was carried out to help unravel the paleogeographic evolution of the Paganzo Basin during Middle Carboniferous–Earliest Permian times. This work is intended to contribute to a more complete understanding of the evolution of the basin by adding detailed information about temporal and spatial changes in the relative participation of the source areas. Taking into account the complex record of marine and nonmarine deposits that integrate the studied interval (Limarino et al., 2002), the impact of sampling different sedimentary environments for a provenance study also is assessed. Finally, an evolutive model to explain the compositional complexities observed in the field is presented.

2. Geologic setting

2.1. Paganzo Basin

The Paganzo Basin (Fig. 1) is one of the largest (about 140,000 km^2) Upper Paleozoic depositional areas recognized along the western margin of Gondwana (Salfity and Gorustovich, 1983; López Gamundí et al., 1994). It can be described as a multihistory basin that shows three main evolutionary stages (Limarino et al., 2003): (1) the foreland stage, developed in an embryonic "proto-Paganzo Basin" during the Protoprecordilleran orogeny; (2) the postorogenic stage, characterized by the widening of the basin, probably as a consequence of the collapse of the Protoprecordillera during the Late Carboniferous–Early Permian (Limarino et al., 2006); and (3) the overfilled stage, characterized by continental deposition during the first stage of the Gondwana breakup (latest Early Permian–Upper Permian).

The complex basement of the Paganzo Basin resulted from the accretion of different terranes during Precambrian–Early to Middle Paleozoic times (Ramos et al., 1986; Ramos, 1988; López Gamundí et al., 1994). Thus, three main morphotectonic elements constitute potential source areas for the sediments of the Paganzo Basin:

1. To the east, the igneous–metamorphic basement of the Sierras Pampeanas and Famatina system (Fig. 1). This "Pampean–Famatinean" basement is formed by plutonic and metamorphic rocks of Ordovician age belonging to the roots of the Famatinean magmatic arc (i.e., Chepes Granite and equivalents). Some sedimentary and low-grade metamorphic rocks of Vendian?–Cambrian age (e.g., Olta Formation) also were partially intruded by these granitoids.
2. The Protoprecordillera in the west-central area (Fig. 1), consisting of Early–Middle Paleozoic clastic and carbonatic sedimentary rocks. It constitutes the mobile belt and is here referred to as the "Protoprecordilleranic" basement.
3. The volcanic and volcaniclastic rocks assigned to the paleo-Pacific magmatic arc of Middle–Late Carboniferous age. These rocks can be found on the northwesternmost edge of the basin, along the border with the Río Blanco Basin (Fig. 1).

The sedimentary filling of the Paganzo Basin is characterized by continental sedimentation to the east and increasing participation of marine deposits to the west (Limarino, 1987; LópezGamundí et al., 1989; Fernández Seveso and Tankard, 1995; Net, 1999; Limarino et al., 2002; Net et al., 2002; Pazos, 2002). Upper Paleozoic strata were included within the Paganzo Group (Bodenbender, 1896; Azcuy and Morelli, 1970b), which was divided into two stratigraphic intervals named the lower (Middle–Late Carboniferous) and upper (Permian) sections (Azcuy and Morelli, 1970b).

Although the lower section of the Paganzo Group traditionally has been considered Middle–Late Carboniferous in age, new stratigraphic and paleontological evidence suggests that its top reached the Earliest Permian (Cisterna and Sabattini, 1998; Cisterna and Simanauskas, 2000; Gutiérrez and Limarino, 2003). Therefore, the time span studied herein goes from Namurian to Early Sakmarian, including the foreland and postorogenic stages of the basin described by Limarino et al. (2003).

2.2. Lower section of the Paganzo group

The lower section of the Paganzo Group includes 200–1200 m of nonmarine and marine clastic sedimentary rocks (sandstones, shales, and some conglomerates) interpreted as alluvial fans, glacial diamictites, and fluvial, deltaic, and shallow marine deposits (e.g., Andreis et al., 1975, 1986; Limarino, 1987; Fauqué and Limarino, 1990; Fernández Seveso et al., 1993; Sterren and Martínez, 1996; Net, 1999; Pazos, 2002; Limarino et al., 2002). In addition, sedimentary rocks are interbedded with volcanic and volcaniclastic rocks at the western boundary of the basin (Aceñolaza, 1971; Fauqué and Limarino, 1990). Thus, the lower section of the Paganzo Group not only covers a large areal extent but also shows lithofacial and compositional changes that resulted in a complex stratigraphic scheme (for a review, see Azcuy and Morelli, 1970b; Limarino et al., 2006) (Fig. 2).

Well-exposed Upper Paleozoic rocks occur at the eastern portion of the basin in the Sierra de Los Llanos area (Andreis et al., 1986; Fig. 1). There, Carboniferous strata filled narrow paleovalleys incised within Lower Paleozoic gneisses, Ordovician granitoids, and low-grade metasedimentary rocks of Vendian? – Cambrian age (i.e., Pampean–Famatinean basement). The lower section of the Paganzo Group was divided in Sierra de Los Llanos into the Malanzán and Loma Larga formations (Andreis et al., 1986). The first unit includes three main intervals: (1) basal conglomerates and diamictites deposited in alluvial fans and periglacial environments; (2) sandstones, shales, and mudstones corresponding to the postglacial transgression of Namurian age (Limarino et al., 2002); and (3) coarse-grained sandstones and conglomerates forming conspicuous Gilbert-type deltaic sequences (Sterren and Martínez, 1996; Net and Limarino, 1999). The Loma Larga Formation consists of conglomerates, sandstones, mudstones, and some coal beds deposited as different styles of fluvial systems (Andreis et al., 1986).

To the northwest, good exposures of the Paganzo Group occur in Sierra de Famatina (Azcuy and Morelli, 1970b; Morelli et al., 1984; Limarino, 1987; Net, 1999) (Fig. 1). In this region, the lower section of the Paganzo Group corresponds to the Lagares Formation (Azcuy and Morelli, 1970b), which rests on granites and high-grade metamorphic rocks of the Famatinean–Pampean basement. The Lagares Formation is mostly composed of fluvial sandstones and conglomerates with conspicuous intercalations of organic-rich mudstones and kaolinitic beds (Di Paola, 1972; Morelli et al., 1984; Limarino, 1987; Net and Limarino, 2000).

Within the Eastern Precordillera and Sierra de Maz areas (Fig. 1), the lower section of the Paganzo Group is divided into the Guandacol and Tupe formations (Andreis et al., 1975). The Guandacol Formation shows a basal interval of glacial-related diamictites that overlies either Ordovician limestones plus fine-grained clastics (in the Precordillera) or Precambrian metamorphic rocks (in Sierra de Maz). Glacial diamictites are followed by shales, fine-grained sandstones, and mudstones deposited during the postglacial transgression in a fjord environment (Limarino et al., 2002). These rocks are conformably covered by the Tupe Formation, made up of conglomerates, cross-bedded sandstones, and thin coal beds that record several types of fluvial systems sporadically interrupted by short marine transgressions (Andreis et al., 1975; Limarino et al., 1986).

Finally, the analyzed interval crops out on the westernmost tip of the Precordillera, at the boundary between the Paganzo and Río Blanco basins. Whereas at Rincón Blanco (Fig. 1), the Punta del Agua and Río del Peñón formations (Aceñolaza, 1971; González and Bossi, 1987) rest on a regional fault above Lower Carboniferous rocks (Net, 1999), a few kilometers to the southeast, in Agua de Carlos (Fig. 1), the Paganzo Group unconformably covers Late Devonian–Early Carboniferous shales of the Jagüel Formation (Fauqué and Limarino, 1990). The Punta del Agua Formation is a volcaniclastic sequence (up to 1000 m thick) that includes andesites, traquites, and dacites, together with lenses of volcanic conglomerates and lithic sandstones (Aceñolaza, 1971; Net, 1999; Remesal et al., 2004); this unit is covered by marine shales of Stephanian age, fluvial sandstones, and sandstone-shale deltaic cycles grouped into the Río del Peñón Formation (Scalabrini Ortiz, 1973; Gutiérrez and Limarino, 2003).

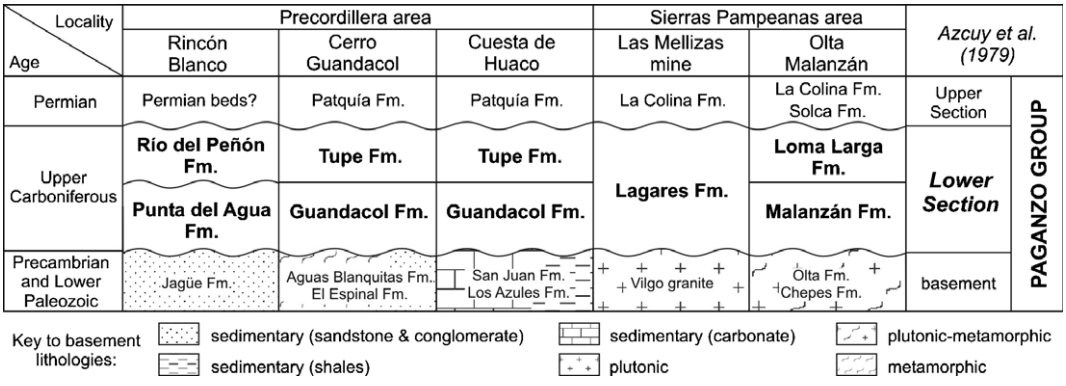

Fig. 2. Lateral correlation of lithostratigraphic units of the lower section of the Paganzo Group between 30° and 31°S latitude (bold). Localities shown in the map of Fig. 1.

2.3. Stratigraphic framework: Depositional intervals

For sampling purposes and provenance interpretations, lithostragraphic units of the lower section of the Paganzo Group were divided into five depositional intervals (DI-1 to DI-5). Depositional intervals are characterized by specific facies arrangements and bounded by regionally correlatable chronostratigraphic surfaces (Figs. 3, 4).

Depositional interval 1 (DI-1) constitutes the basal infill of the Paganzo Basin (Fig. 3). It ranges in thickness from a few to 90 m, occurring throughout the basin but usually as laterally discontinuous units that fill isolated paleovalleys (Andreis et al., 1986). DI-1 consists of coarse-grained conglomerates, sandstones, and diamictites deposited in alluvial fans, proximal braided rivers, and glacial environments (Andreis et al., 1986; Limarino, 1987; Marenssi et al., 2002). Glaciolacustrine deposits intercalated into glacial diamictites have yielded palynological assemblages of Namurian age (Limarino and Gutiérrez, 1990; César and Gutiérrez, 2000).

A regional marine flooding surface divides the coarse-grained deposits included in DI-1 from dropstone-bearing shales, fine-grained sandstones, resedimented diamictites,

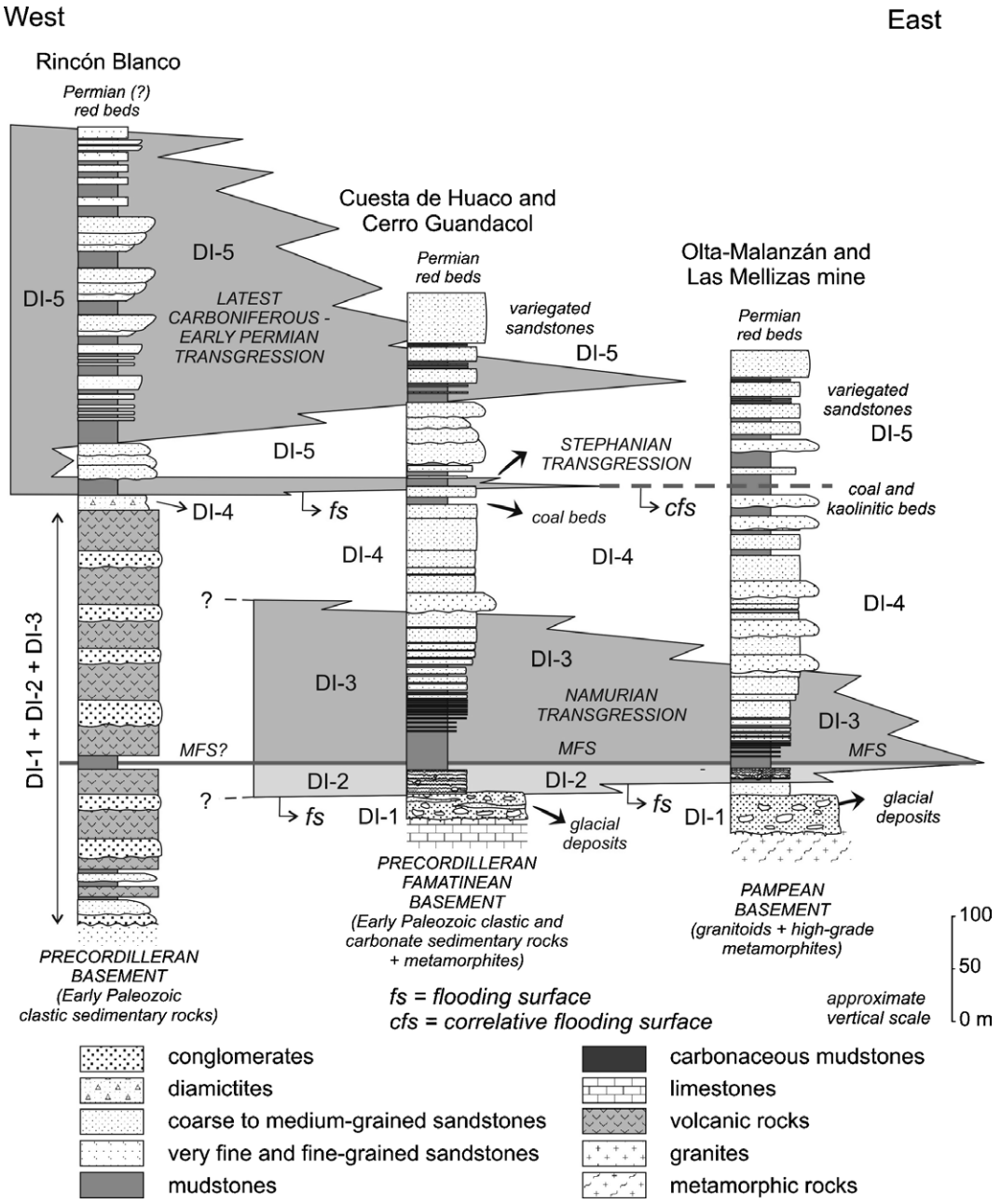

Fig. 3. Integrated profiles of localities included this work showing regionally correlatable chronostratigraphic surfaces that delineate depositional intervals (DI-1 to DI-5).

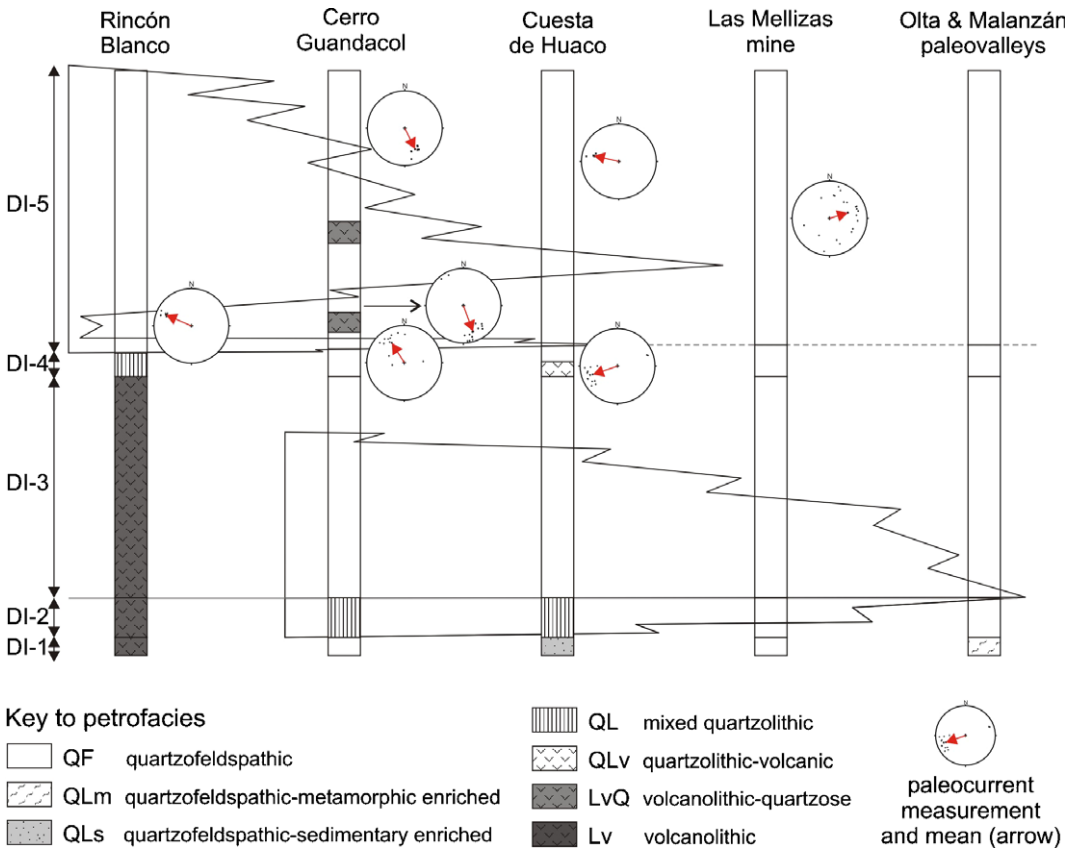

Fig. 4. Schematic logs (not to scale) showing petrofacies distribution and unpublished paleocurrent data (Net, 1999). Chronostratigraphic surfaces as in Fig. 3.

and thin beds of marls grouped as depositional interval 2 (DI-2) (Fig. 3). DI-2 rocks are interpreted as the transgressive system track (TST) of the postglacial Namurian transgression, recognized not only in the Paganzo but also in the neighboring Río Blanco and Calingasta–Uspallata basins (Limarino et al., 2002).

The maximum flooding surface (MFS) of the Namurian transgression marks the beginning of depositional interval 3 (DI-3) (Fig. 3). DI-3 comprises a basal shale-rich section (deposited during the maximum flooding stage), followed by sandstones and conglomerates deposited later as prograding fluviodeltaic deposits during the highstand stage. The nature of DI-3 deposits is controlled by the paleogeography of the basin; whereas in the eastern Paganzo Basin, Gilbert-type deltas and fluviodeltaic sequences prevailed (Sterren and Martínez, 1996; Net and Limarino, 1999), large deltas with thickening- and coarsening-upward patterns formed in western Paganzo Basin (Limarino et al., 2002). Palynological associations including achritarcs in the Malanzán Formation suggest a Namurian age for this interval (Gutiérrez and Limarino, 2001).

Depositional interval 4 (DI-4) comprises an extensive blanket (up to 180 m thick) of conglomerates, coarse-grained sandstones, and shales of fluvial origin that transitionally covers the marine and deltaic deposits throughout the basin (Limarino et al., 1986; Fernández Seveso et al., 1993) (Fig. 3). Although this depositional interval could represent the late (aggradational) stage of the highstand system track (HST), it more probably is associated with the inland expression of the forced regression described in the neighboring Calingasta–Uspallata Basin by Buatois and Limarino (2003). The age of the DI-4 can be constrained by the presence of plant remains belonging to Middle—Upper Carboniferous NBG flora (Archangelsky et al., 1996) and palynological assemblages of sub-biozone A of the *Raistrickia densa-Convolutispora muriornata* biozone of Upper Carboniferous age (César and Gutiérrez, 2000).

A second flooding surface restricted to the western portion of the Paganzo Basin marks the base of depositional interval 5 (DI-5). This stratigraphic level (up to 100 m) comprises shales, fine-grained sandstones, and some marls deposited in coastal and shelf environments, though some intercalations of conglomerates and coarse-grained sandstones reflecting punctuated episodes of fluvial sedimentation are also included. These marine sediments pinch out to the east into fluvial sandstones and conglomerates deposited in both low- and high-sinuosity rivers (Limarino, 1987). Sea-level changes taking place in the western marine domain are reflected in the eastern inland area by changes in flood-basin preservation and channel geometry of fluvial deposits (Limarino, 1987; Net, 1999). Both marine invertebrates (Sabattini et al., 1991; Archangelsky et al., 1996) and

radimetric ages (Fauqué et al., 1999) indicate that DI-5 has a Latest Carboniferous–Earliest Permian age.

This model appears partially masked by the volcanic activity that characterizes the Punta del Agua Formation (Aceñolaza, 1971; Remesal et al., 2004) in the westernmost Rincón Blanco section (Fig. 1). Thus, DI-1, DI-2, and DI-3 deposits often occur as discontinuous clastic wedges laterally replaced by volcanic and volcaniclastic rocks (Fig. 3).

3. Petrographic methods

Sampling localities were selected to represent the main morphotectonic elements that constitute the basement of the Paganzo Basin. A total of 187 sandstone samples of the Lagares, Malanzán, Loma Larga, Guandacol, Tupe, Punta del Agua, and Río del Peñón formations from five localities are included in this work (Table 1). During sampling, sandstones were assigned to their depositional interval (DI-1 to DI-5).

In a parallel way, the paleodrainage system of the studied deposits was examined using data published by previous authors (Spalletti, 1968; Andreis et al., 1975; Andreis et al., 1986; LópezGamundí et al., 1989; Sterren and Martínez, 1996), together with unpublished paleocurrent measurements obtained from medium- and large-scale cross-bedded sandstones in fluvial and fluviodeltaic intervals (Net, 1999; Fig. 4).

Sandstone samples were thin sectioned and point counted (300–500 points per sample), following the Gazzi–Dickinson methodology (Zuffa, 1985), to minimize compositional variabilities due to grain size. Pervasively altered sandstones and those with significant amounts of altered grains (>10%) were excluded from the data set. Detrital modes were obtained after reassigning framework grains to the QFL and QmFLt categories (Table 2). Provenance discriminations are based on schemes by Dickinson et al. (1983) and consider the hierarchy of different depositional environments for provenance interpretations defined by Ingersoll et al. (1993).

Table 1
Summary of point-count data of sandstones from the Lower Section of the Paganzo Group

	Grain composition (recalculated to 100% of the framework fraction)[a]												
	Qm	Qp	Ch	FK	Plg	Lm	Lvi	Lvm	Lvf	Lvv	Ls	C	Otr
Eastern domain													
Olta-Malanzán													
DI-1 ($n=3$)	33 ± 2	0 ± 0	0 ± 0	14 ± 6	13 ± 8	21 ± 4	0 ± 0	0 ± 0	1 ± 1	0 ± 0	0 ± 0	0 ± 0	4 ± 1
DI-2 ($n=14$)	42 ± 6	0 ± 1	0 ± 0	15 ± 6	8 ± 4	5 ± 6	0 ± 0	0 ± 0	0 ± 0	0 ± 0	0 ± 0	0 ± 0	4 ± 2
DI-3 ($n=5$)	37 ± 5	0 ± 0	0 ± 0	11 ± 4	12 ± 3	5 ± 3	0 ± 0	0 ± 0	0 ± 0	0 ± 0	0 ± 0	0 ± 0	10 ± 3
DI-4 ($n=3$)	30 ± 3	0 ± 1	0 ± 0	20 ± 5	12 ± 3	9 ± 5	0 ± 0	0 ± 0	0 ± 0	0 ± 0	2 ± 3	0 ± 0	10 ± 5
DI-5 ($n=3$)	40 ± 6	1 ± 0	0 ± 0	12 ± 3	2 ± 1	3 ± 1	0 ± 0	0 ± 0	0 ± 0	0 ± 0	0 ± 0	0 ± 0	11 ± 2
Las Mellizas mine													
DI-1 ($n=5$)	53 ± 5	1 ± 0	0 ± 0	16 ± 3	0 ± 1	0 ± 0	0 ± 0	0 ± 0	0 ± 0	0 ± 0	0 ± 0	0 ± 0	4 ± 1
DI-2 ($n=1$)	55	1	0	10	0	1	0	0	0	0	0	0	5
DI-3 ($n=3$)	56 ± 6	1 ± 1	0 ± 0	11 ± 5	0 ± 0	0 ± 0	0 ± 0	0 ± 0	0 ± 0	0 ± 0	0 ± 0	0 ± 0	3 ± 1
DI-4 ($n=4$)	57 ± 6	1 ± 0	0 ± 0	11 ± 5	0 ± 0	0 ± 1	0 ± 0	0 ± 0	0 ± 0	0 ± 0	0 ± 0	0 ± 0	11 ± 8
DI-5 ($n=6$)	54 ± 8	3 ± 2	0 ± 0	13 ± 5	0 ± 0	1 ± 1	0 ± 0	0 ± 0	0 ± 0	0 ± 0	0 ± 0	0 ± 0	7 ± 4
Western domain													
Cuesta de Huaco													
DI-1 ($n=8$)	31 ± 5	1 ± 1	0 ± 0	7 ± 2	6 ± 2	1 ± 1	0 ± 0	0 ± 0	0 ± 0	0 ± 0	5 ± 6	2 ± 2	5 ± 2
DI-2 ($n=8$)	23 ± 3	1 ± 1	0 ± 0	8 ± 3	1 ± 1	2 ± 2	0 ± 0	0 ± 0	0 ± 0	0 ± 0	1 ± 1	0 ± 0	6 ± 2
DI-3 ($n=19$)	39 ± 8	1 ± 1	0 ± 0	17 ± 6	3 ± 1	1 ± 1	0 ± 0	0 ± 0	0 ± 0	0 ± 0	0 ± 0	0 ± 0	8 ± 4
DI-4 (ark) ($n=4$)	44 ± 5	1 ± 1	0 ± 0	18 ± 10	10 ± 7	3 ± 2	0 ± 0	0 ± 1	0 ± 0	0 ± 0	0 ± 0	0 ± 0	3 ± 1
DI-4 (volc) ($n=7$)	41 ± 7	2 ± 1	13 ± 8	9 ± 2	3 ± 2	1 ± 1	0 ± 0	8 ± 4	1 ± 2	1 ± 1	2 ± 1	0 ± 0	2 ± 2
DI-5 ($n=12$)	51 ± 10	2 ± 1	0 ± 0	15 ± 7	3 ± 3	1 ± 2	0 ± 0	0 ± 0	0 ± 0	0 ± 0	0 ± 0	0 ± 0	4 ± 2
Cerro Guandacol													
DI-1 ($n=2$)	48 ± 2	1 ± 0	0 ± 0	21 ± 2	7 ± 2	3 ± 2	0 ± 0	1 ± 0	1 ± 1	0 ± 0	1 ± 1	0 ± 0	1 ± 1
DI-2 ($n=6$)	30 ± 15	2 ± 1	1 ± 1	8 ± 4	3 ± 1	25 ± 19	0 ± 0	7 ± 11	1 ± 1	0 ± 0	1 ± 3	0 ± 0	4 ± 3
DI-3 ($n=16$)	45 ± 7	1 ± 1	0 ± 0	17 ± 6	12 ± 7	3 ± 2	0 ± 0	0 ± 0	0 ± 0	0 ± 0	0 ± 0	0 ± 0	5 ± 3
DI-4 ($n=9$)	57 ± 6	1 ± 0	0 ± 0	10 ± 3	15 ± 3	3 ± 1	0 ± 0	2 ± 3	0 ± 0	0 ± 0	0 ± 0	0 ± 0	1 ± 1
DI-5 (ark) ($n=9$)	54 ± 9	1 ± 1	0 ± 0	11 ± 4	13 ± 8	1 ± 1	0 ± 0	0 ± 0	0 ± 1	0 ± 0	0 ± 1	0 ± 0	2 ± 2
DI-5 (volc) ($n=6$)	34 ± 13	2 ± 2	1 ± 0	6 ± 2	4 ± 2	7 ± 4	0 ± 0	22 ± 11	1 ± 1	0 ± 0	0 ± 0	0 ± 0	4 ± 2
Rincón Blanco													
DI-1 to DI-3 ($n=12$)	15 ± 3	1 ± 1	0 ± 1	9 ± 9	10 ± 3	4 ± 2	3 ± 8	6 ± 6	21 ± 14	13 ± 7	0 ± 1	0 ± 0	2 ± 2
DI-4 ($n=4$)	37 ± 8	1 ± 1	1 ± 1	8 ± 1	10 ± 2	5 ± 2	0 ± 0	2 ± 1	1 ± 0	0 ± 0	0 ± 0	0 ± 0	1 ± 1
DI-5 ($n=10$)	59 ± 7	2 ± 1	1 ± 0	6 ± 3	11 ± 6	2 ± 1	0 ± 0	0 ± 0	0 ± 1	0 ± 0	0 ± 1	0 ± 0	3 ± 2

[a] Key to grain types: Qm=monocrystalline quartz; Qp=polycrystalline quartz; Ch=chert; FK=K-feldspar; Plg=plagioclase; Lm=methamorphic rock fragment; Lvi/m/f/v=volcanic rock fragment lathwork/micrlitic/felsitic/vitric; Ls=sedimentary rock; fragment (clastic); C=carbonate rock fragment; Otr=others (accessory minerals, altered grains).

Table 2
Detrital modes and grain-type ratios for sandstones of the lower section of the Paganzo Group

	Dickinson et al. (1983)[a]						Grain parameters[b]						PTF[c]
	Q	F	L	Qm	F	Lt	Qp/Qm	Plg/FK	Lm/Lt	Lv+Ls/Lt	Lv/Lt	Ls/Lm	
Eastern domain													
Olta-Malanzán													
DI-1 ($n = 3$)	41 ± 3	33 ± 2	26 ± 4	40 ± 2	33 ± 2	27 ± 4	0.01 ± 0.01	1.21 ± 0.87	0.97 ± 0.05	0.03 ± 0.05	0.03 ± 0.05	0.00 ± 0.00	QF-Lm
DI-2 ($n = 14$)	61 ± 9	32 ± 7	7 ± 8	60 ± 9	32 ± 7	8 ± 8	0.01 ± 0.01	0.70 ± 0.45	0.99 ± 0.01	0.01 ± 0.01	0.00 ± 0.00	0.01 ± 0.01	QF
DI-3 ($n = 5$)	57 ± 6	35 ± 6	8 ± 4	56 ± 6	35 ± 6	9 ± 4	0.02 ± 0.01	1.28 ± 0.46	1.00 ± 0.00	0.00 ± 0.00	0.00 ± 0.00	0.00 ± 0.00	QF
DI-4 ($n = 3$)	42 ± 7	44 ± 6	14 ± 8	41 ± 8	44 ± 6	15 ± 8	0.02 ± 0.02	0.61 ± 0.20	0.87 ± 0.22	0.13 ± 0.22	0.00 ± 0.00	0.21 ± 0.36	QF
DI-5 ($n = 3$)	71 ± 2	24 ± 0	5 ± 2	69 ± 2	24 ± 0	7 ± 2	0.03 ± 0.00	0.24 ± 0.15	0.92 ± 0.13	0.08 ± 0.13	0.05 ± 0.09	0.03 ± 0.06	QF
Las Mellizas mine													
DI-1 ($n = 5$)	76 ± 5	24 ± 5	0 ± 0	75 ± 5	24 ± 5	1 ± 1	0.02 ± 0.01	0.03 ± 0.05	–	–	–	–	QF
DI-2 ($n = 1$)	84	15	1	82	15	3	0.02	0.00	1.00	0.00	0.00	0.00	QF
DI-3 ($n = 3$)	83 ± 7	17 ± 7	0 ± 0	82 ± 7	17 ± 7	1 ± 0	0.01 ± 0.01	0.04 ± 0.07	1.00 ± 0.00	0.00 ± 0.00	0.00 ± 0.00	0.00 ± 0.00	QF
DI-4 ($n = 4$)	84 ± 7	16 ± 7	1 ± 1	83 ± 7	16 ± 7	2 ± 1	0.01 ± 0.01	0.00 ± 0.00	1.00 ± 0.00	0.00 ± 0.00	0.00 ± 0.00	0. 00 ± 0.00	QF
DI-5 ($n = 6$)	80 ± 8	18 ± 7	1 ± 1	75 ± 11	18 ± 7	6 ± 4	0.07 ± 0.05	0.02 ± 0.04	1.00 ± 0.00	0.00 ± 0.00	0.00 ± 0.00	0.00 ± 0.00	QF
Western domain													
Cuesta de Huaco													
DI-1 ($n = 8$)	62 ± 9	24 ± 3	14 ± 8	60 ± 9	24 ± 3	16 ± 8	0.03 ± 0.02	0.88 ± 0.38	0.11 ± 0.13	0.89 ± 0.13	0.00 ± 0.00	13.28 ± 8.69	QF-Ls
DI-2 ($n = 8$)	67 ± 7	24 ± 7	9 ± 5	64 ± 6	24 ± 7	12 ± 5	0.04 ± 0.03	0.18 ± 0.06	0.61 ± 0.29	0.39 ± 0.29	0.00 ± 0.00	2.49 ± 5.48	QL
DI-3 ($n = 19$)	65 ± 10	33 ± 10	1 ± 1	64 ± 9	33 ± 10	3 ± 2	0.02 ± 0.02	0.18 ± 0.06	0.93 ± 0.26	0.07 ± 0.26	0.00 ± 0.00	–	QF
DI-4 (ark) ($n = 4$)	60 ± 6	36 ± 10	4 ± 5	57 ± 6	36 ± 10	6 ± 5	0.04 ± 0.02	0.92 ± 0.90	0.93 ± 0.14	0.07 ± 0.14	0.05 ± 0.09	0.03 ± 0.06	QF
DI-4 (volc) ($n = 7$)	69 ± 6	14 ± 3	17 ± 6	50 ± 8	14 ± 3	35 ± 11	0.39 ± 0.21	0.34 ± 0.23	0.11 ± 0.05	0.89 ± 0.05	0.76 ± 0.05	1.62 ± 1.20	QLv
DI-5 ($n = 12$)	74 ± 12	24 ± 12	2 ± 2	71 ± 13	24 ± 12	5 ± 3	0.04 ± 0.02	0.22 ± 0.24	0.77 ± 0.36	0.23 ± 0.36	0.11 ± 0.30	0.43 ± 0.92	QF
Cerro Guandacol													
DI-1 ($n = 2$)	60 ± 1	34 ± 5	6 ± 4	59 ± 1	34 ± 5	7 ± 4	0.02 ± 0.00	0.33 ± 0.06	0.66 ± 0.15	0.34 ± 0.15	0.27 ± 0.06	0.12 ± 0.17	QF
DI-2 ($n = 6$)	43 ± 22	15 ± 8	42 ± 29	40 ± 21	15 ± 8	45 ± 29	0.09 ± 0.05	0.41 ± 0.20	0.74 ± 0.16	0.26 ± 0.16	0.22 ± 0.16	0.06 ± 0.10	QL
DI-3 ($n = 16$)	59 ± 6	37 ± 8	4 ± 4	58 ± 4	37 ± 8	5 ± 5	0.02 ± 0.03	0.90 ± 0.73	0.93 ± 0.07	0.07 ± 0.07	0.07 ± 0.07	0.00 ± 0.02	QF
DI-4 ($n = 9$)	66 ± 5	28 ± 3	6 ± 6	65 ± 5	28 ± 3	7 ± 6	0.02 ± 0.01	1.94 ± 1.45	0.63 ± 0.18	0.37 ± 0.18	0.29 ± 0.22	0.13 ± 0.10	QF
DI-5 (ark) ($n = 9$)	67 ± 9	30 ± 8	3 ± 2	66 ± 8	30 ± 8	4 ± 3	0.02 ± 0.01	1.53 ± 1.34	0.63 ± 0.43	0.37 ± 0.43	0.19 ± 0.25	0.29 ± 0.58	QF
DI-5 (volc) ($n = 6$)	47 ± 17	13 ± 5	39 ± 19	43 ± 16	13 ± 5	43 ± 19	0.09 ± 0.06	0.72 ± 0.35	0.23 ± 0.05	0.77 ± 0.05	0.76 ± 0.05	0.04 ± 0.06	LvQ
Rincón Blanco													
DI-1 to DI-3 ($n = 12$)	20 ± 4	23 ± 12	58 ± 13	18 ± 3	23 ± 12	59 ± 13	0.09 ± 0.08	5.28 ± 10.67	0.08 ± 0.04	0.92 ± 0.04	0.91 ± 0.05	0.12 ± 0.24	Lv
DI-4 ($n = 4$)	60 ± 5	28 ± 2	12 ± 4	57 ± 5	28 ± 2	15 ± 4	0.05 ± 0.01	1.23 ± 0.24	0.68 ± 0.21	0.32 ± 0.21	0.32 ± 0.21	0.00 ± 0.00	QL
DI-5 ($n = 10$)	76 ± 9	21 ± 10	3 ± 2	73 ± 9	21 ± 10	6 ± 3	0.04 ± 0.02	1.90 ± 1.33	0.80 ± 0.17	0.20 ± 0.17	0.12 ± 0.12	0.13 ± 0.25	QF

[a] Q, total quartz; Qm, monocrystalline quartz; F, total feldspar; L, rock fragments; and Lt, total rock fragments (including polycrystalline quartz).
[b] Qm/p, monocrystalline/polycrystalline quartz; FK, K–feldspar; Plg, plagioclase; and Lm/v/s/t, metamorphic/volcanic/sedimentary/total rock fragments.
[c] PTF, petrofacies (see text for code explanation).

4. Sandstone petrography

Sandstones from the lower section of the Paganzo Group exhibit significant variability in both texture and composition (Net, 1999). Samples included in the data set (Table 1) range from very coarse to fine grained. Although matrix content is generally low (0–15%), some sandstones, particularly within glacigenic levels, have significant amounts of interstitial material (15–50%). Matrix-rich sandstones are included in the data set because the matrix has been interpreted as recrystallized detrital (i.e., ortomatrix; Dickinson, 1970), whereas epimatrix and pseudomatrix (*sensu* Dickinson, 1970) seem rare.

Compositional varieties of sandstones are dominated by arkose and subarkose, whereas litharenites, lithic arkose, feldspathic litharenite, and sublitharenite occur at specific stratigraphic levels (Net, 1999). Framework grains can be divided into quartzose (Q), feldspar (F), and lithic fragments (L) (Dickinson, 1970). Monocrystalline quartz of plutonic/metamorphic origin (Qm) constitutes the most abundant grain type. Polycrystalline quartz is scarce, though it can be locally abundant in some sandstones of the Guandacol and Punta del Agua formations. Two types of polycrystalline quartz have been distinguished: (1) metamorphic/mylonitic (Qp), with relatively large subgrains (4–62 μm) and common sutured contacts among them, and (2) chert (Ch), composed of microquartz with minute subgrains (<4 μm), megaquartz, opal, and chalcedony. Feldspar grains include both K–feldspar (KF, microcline, and orthoclase) and plagioclase (Plg). Rock fragments group metamorphic (Lm), volcanic (Lv), and sedimentary (Ls) varieties. Metamorphic rock fragments include schist, gneiss, amphibolites, and metavolcanics. Volcanic rock fragments include lathwork grains (Lvl) with intergranular/intersertal texture; microlithic grains (Lvm) with pilotaxitic, felted, trachitic, and hyalopilitic textures; felsitic grains (Lvf) composed of quartz and feldspar intergrowths; and vitric grains (Lvv) that include vitrophyric textures and tuff fragments. Finally, sedimentary rock fragments include both clastic (Ls) and carbonate (C) varieties. Clastic sedimentary rock fragments comprise shale, siltstone, and very fine-grained sandstones. Carbonate grains are mudstone and wackestone fragments showing bioclasts and recrystallization veins that identify them as "extrabasinal carbonate" (CE) (Zuffa, 1980, 1985; Mack, 1984); as will be discussed subsequently, CE grains provide critical information regarding the Precordillera as a source area.

Main diagenetic alterations in these sandstones include: (1) feldspar dissolution, kaolinitization/illitization, and albitization (Net, 1999; Net and Limarino, 2000); (2) selective chloritization of rock fragments; and (3) grain replacement and concomitant secondary porosity generation (Di Paola, 1972; Andreis et al., 1986; Net, 1999). In all cases, replaced and/or dissolved grains were restored and point counted as the precursor grain for provenance interpretation.

5. Petrofacies

The term petrofacies was coined to refer to sandstones of similar composition, usually defined by parameters such as QFL percentages and/or the ratio of different grain types (Mansfield, 1971; Dickinson and Rich, 1972). Petrofacies delineate stratigraphic entities that can be referred to as petrologic intervals (Dickinson and Rich, 1972). Analysis of the vertical variation in sandstone detrital modes within the Lower Paganzo Group distinguishes seven petrofacies: quartzofeldespathic (QF), quartzolithic-metamorphic (QLm), quartzolithic-sedimentary (QLs), mixed quartzolithic (QL), quartzolithic-volcanic (QLv), volcanolithic-quartzose (LvQ), and volcanolithic (Lv) (Tables 2 and 3).

5.1. Quartzofeldespathic (QF) petrofacies

The quartzofeldespathic (QF) petrofacies (Q 67 ± 12 F 29 ± 10 L 4 ± 5, Qm 66 ± 11 F 29 ± 10 Lt 5 ± 5) includes typical arkose (Fig. 5a). These sandstones have moderate to high monocrystalline quartz content, very low polycrystalline quartz (Qp/Qm < 0.1), and abundant feldspar grains, with K–feldspar (particularly microcline) clearly dominant over plagioclase (FK > Plg), whereas lithic

Table 3
Summary of compositional characteristics of the petrofacies defined in this work

Petrofacies name	Code	Detrital modes	Interpreted source (s) area(s)[a]	Petrosome
Quartzofeldespathic	QF	Q 67 ± 12 F 29 ± 10 L 4 ± 5 Qm 66 ± 11 F 29 ± 10 Lt 5 ± 5	PFb	Basement
Quartzolithic-metamorphic enriched	QF-Lm	Q 41 ± 3 F 33 ± 2 L 26 ± 4 Qm 40 ± 2 F 33 ± 2 Lt 27 ± 4	PFb	Basement
quartzolithic-sedimentary enriched	QF-Ls	Q 62 ± 9 F 24 ± 3 L 14 ± 8 Qm 60 ± 9 F 24 ± 3 Lt 16 ± 8	PPC	Recycled orogen
Mixed quartzolithic	QL	Q 58 ± 17 F 22 ± 8 L 21 ± 23 Qm 54 ± 16 F 22 ± 8 Lt 24 ± 22	PFb ± PPC ± CVA	Recycled orogen
Quartzolithic-volcanic	QLv	Q 69 ± 6 F 14 ± 3 L 17 ± 6 Qm 50 ± 8 F 14 ± 3 Lt 35 ± 11	CVA + PC	Volcanic arc
Volcanolithic-quartzose	LvQ	Q 47 ± 17 F 13 ± 5 L 39 ± 19 Qm 43 ± 16 F 13 ± 5 Lt 43 ± 19	CVA + PFb	Volcanic arc
Volcanolithic	Lv	Q 20 ± 4 F 23 ± 12 L 58 ± 13 Qm 18 ± 3 F 23 ± 12 Lt 59 ± 13	CVA	Volcanic arc

[a] Key to source areas: PFb, Pampean–Famatinean basement; PPC, Protoprecordillera; and CVA, Carboniferous Volcanic Arc.

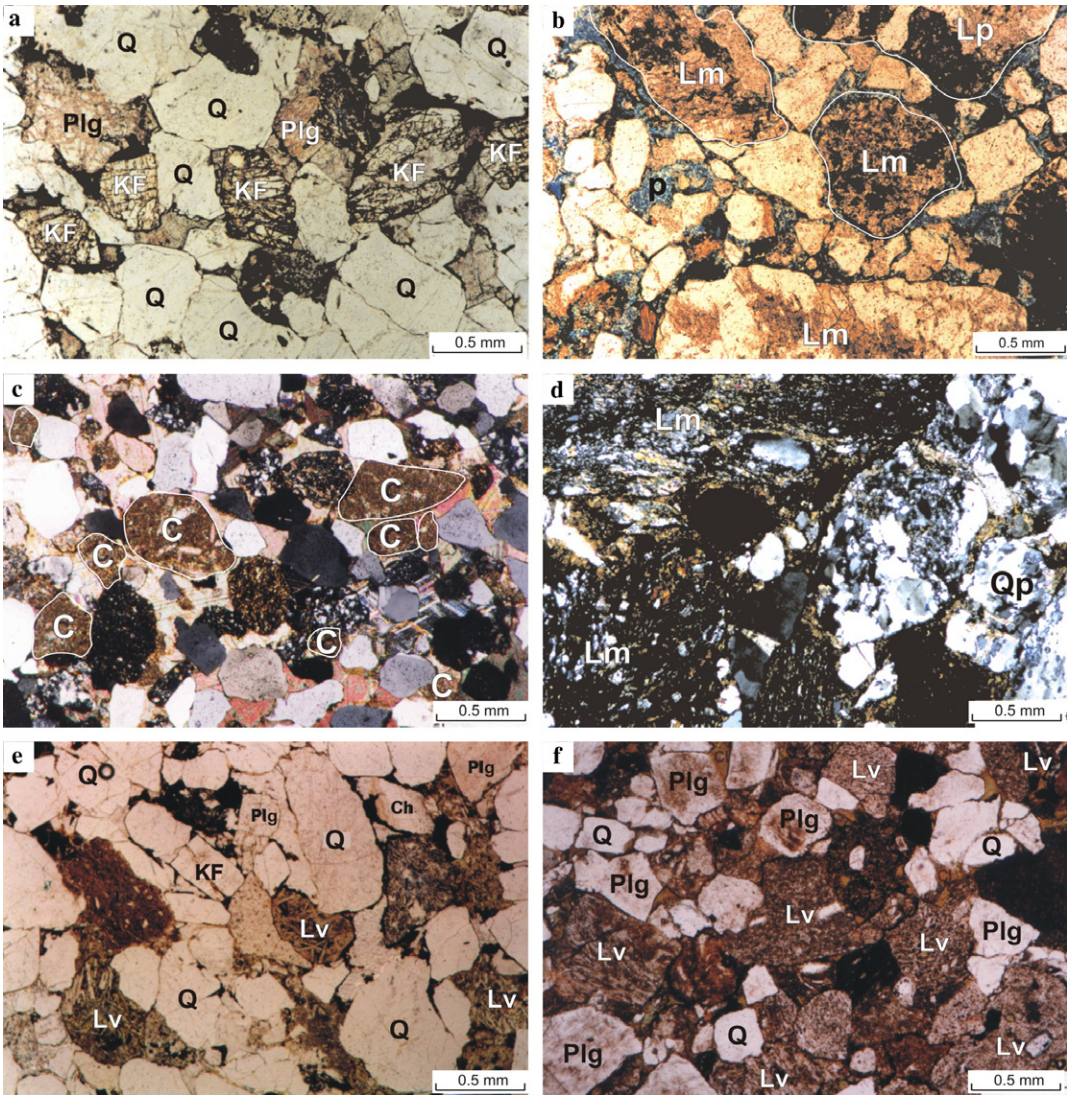

Fig. 5. Compositional variation of studied sandstones as reflected by different petrofacies: (a) QF petrofacies, note abundant quartz (Q), k–feldspar (KF, stained yellow), and plagioclase grains (P, stained pink), sample T31, Tupe Formation, Cuesta de Huaco. (b) QF-Lm petrofacies, characterized by less quartz and abundant metamorphic (Lm) and common plutonic (Lp) grains, pore space in blue (p), sample MA24, Malanzán Formation, Olta paleovalley. (c) QF-Ls petrofacies, with common extraformational carbonate grains (C), sample 64, Guandacol Formation, Cuesta de Huaco. (d) QL petrofacies, with variety of lithic (e.g., metamorphic, Lm) grains and polycrystalline quartz (Qp), sample CG24, Guandacol Formation, Cerro Guandacol. (e) QLv petrofacies with common quartz (Q) and volcanic rock fragments (Lv), minor k–feldspar (KF), some plagioclase (P), and chert (Ch), sample T8, Tupe Formation, Cuesta de Huaco. (f) Lv petrofacies with abundant volcanic rock fragments (Lv) and plagioclase grains (P) but minor quartz (Q), sample PA5, Punta del Agua Formation, Rincón Blanco. All photomicrographs X40; (a, b, e, and f) plain light; (c and d) crossed polars.

content is very low (L < 10%). The relative enrichment in quartz content in sandstones of the QF petrofacies from the Lagares Formation at Las Mellizas mine (Table 2) is due to feldspar kaolinitization (Di Paola, 1972; Net, 2002).

QF petrofacies is volumetrically the most common petrofacies in Carboniferous deposits of the Paganzo Basin. It is particularly dominant in the eastern domain of the basin (i.e., Olta-Malanzán and Las Mellizas mine localities; Fig. 1), where it has been identified in all depositional intervals (DI-1 to DI-5; Fig. 4). To the west, QF petrofacies thins upward as a progradational wedge of arkosic composition and interfingers with other petrofacies (Fig. 4).

QF sandstones reflect a continental block provenance signature (Fig. 6), indicating they are sourced from the granitic/high-metamorphic basement that constitutes the Sierras Pampeanas and/or Sierra de Famatina (Fig. 1). Paleocurrents measured within QF intervals agree with this input from easterly located crystalline rocks (Andreis et al., 1975, 1986; Sterren and Martınez, 1996; Net, 1999; Fig. 4).

5.2. Quartzofeldespathic-metamorphic enriched (QF-Lm) petrofacies

The quartzofeldespathic-metamorphic enriched QF(Lm) petrofacies (Q 41 ± 3 F 33 ± 2 L 26 ± 4, Qm 40 ± 2 F 33 ± 2 Lt 27 ± 4) is characterized by intermediate to low quartz content, low polycrystalline quartz (Qp/Qm < 0.1), plagioclase grains that dominate over K–feldspars

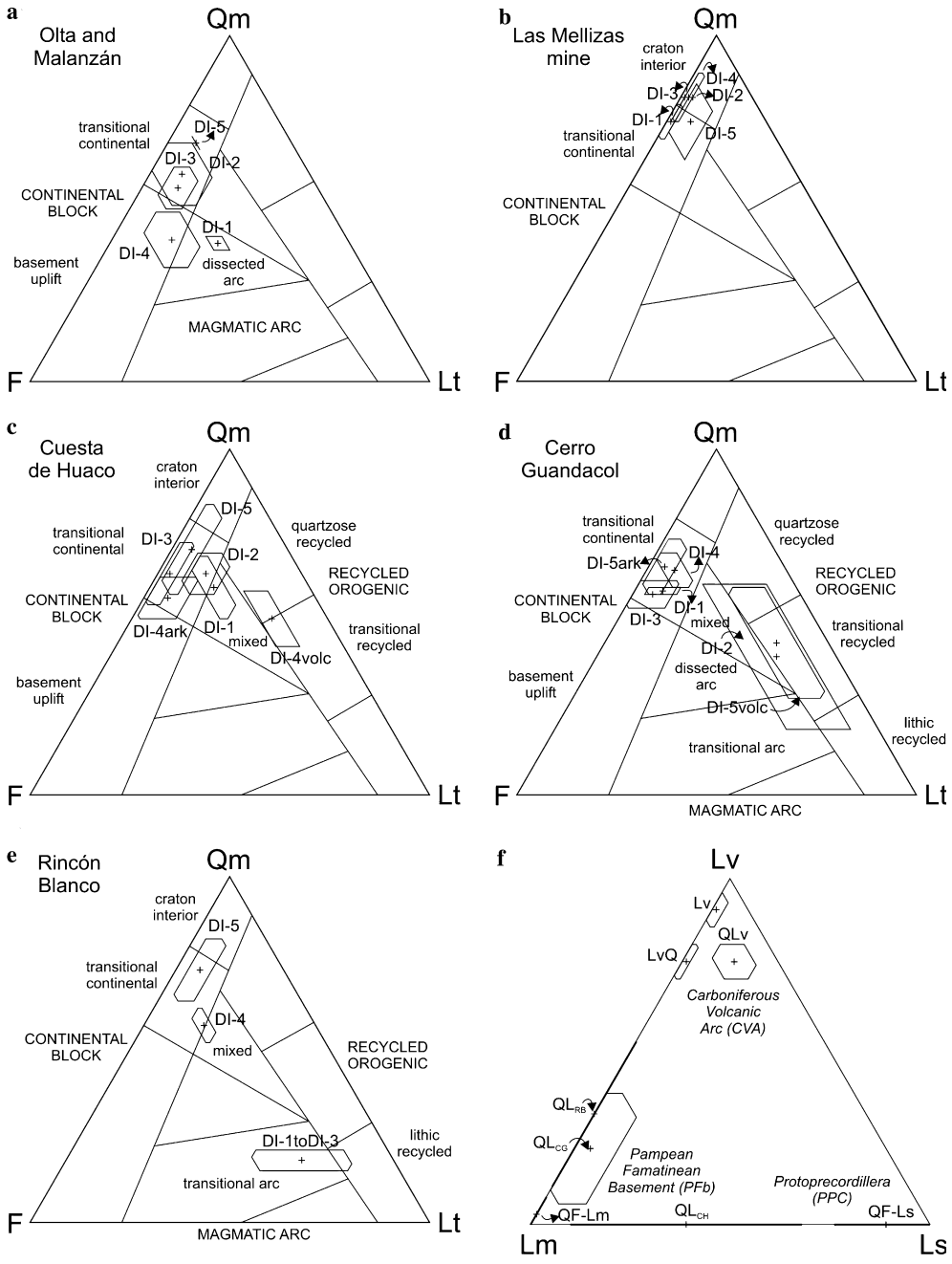

Fig. 6. QmFLt detrital modes of sandstones for each depositional interval (DI-1 to DI-5) from (a) Olta and Malanzán paleovalleys; (b) Las Mellizas mine; (c) Cuesta de Huaco; (d) Cerro Guandacol; and (e) Rincón Blanco. (f) LvLmLs triangle for all other-than-continental-block-provenance petrofacies showing relative participation of each source area. Provenance diagrams after Dickinson et al. (1983).

(Plg/FK > 1), and abundant metamorphic rock fragments (Lm/Lt near 1; Fig. 5b, Table 2).

QLm petrofacies is only present in the eastern domain of the Paganzo Basin, where schist and phyllites locally constitute the Pampean–Famatinean basement (i.e., Olta and Malanzán paleovalleys, Fig. 4). QLm sandstones are the matrix of conglomerates in lateral alluvial fans that result in the basal fill of the Malanzán paleovalley (DI-1). These alluvial fans exhibit the characteristic radial pattern of paleocurrents usually described for that depositional environment (Sterren and Martínez, 1996). QLm petrofacies thus reflects regions in which the plutonic-metamorphic Pampean–Famatinean basement is locally dominated by tonalites and low-grade metamorphic rocks.

Although geologic evidence clearly points to a continental block as the provenance area for these QLm sandstones, their detrital modes plot in the dissected arc provenance field of Dickinson et al. (1983) (DI-1 in Fig. 6a). This apparent mismatch results from the high content of fine-grained, low-grade metamorphic rock fragments that shift the composition toward the Lt (total lithic fragments) pole of the triangle. It also should be noted that alluvial fan

sandstones belong to the first-order sampling scale of Ingersoll et al. (1993), which is appropriate only to assess the nature of local source rocks and not to interpret regional tectonic settings (e.g., sandstones from higher sampling orders are from big rivers and deltas or shorezone; Ingersoll et al., 1993).

5.3. Quartzofeldespathic-sedimentary enriched (QF-Ls) petrofacies

The quartzofeldespathic-sedimentary enriched (QF(Ls)) petrofacies (Q 62 ± 9 F 24 ± 3 L 14 ± 8, Qm 60 ± 9 F 24 ± 3 Lt 16 ± 8) can be defined by its moderate quartz content, low polycrystalline quartz (Qp/Qm < 0.1), low to moderate plagioclase content (Plg/FK $= 0.5$–1), and particularly the dominance of sedimentary rock fragments (clastic or extraformational carbonatic) over metamorphic rock fragments (Ls/Lm $\gg 1$; Fig. 5c, Table 2).

QLs petrofacies is restricted to DI-1 in localities where sandstones directly overlie Early Paleozoic sediments of the Precordillera (e.g., Cuesta de Huaco; Figs. 3, 4). Abundance of limestones and fine-grained clastic sedimentary rock fragments in these sandstones points out to a mixed provenance signal that reflects the input from the Precordilleranic basement (DI-1 in Fig. 6c).

5.4. Mixed quartzolithic (QL) petrofacies

The mixed quartzolithic (QL) petrofacies (Q 58 ± 17 F 22 ± 8 L 21 ± 23, Qm 54 ± 16 F 22 ± 8 Lt 24 ± 22) is characterized by its moderate to high total quartz content, with variable amounts of polycrystalline quartz (Qp/Qm near 0.05). Relative amounts of K–feldspar and plagioclase are variable (Plg/FK $= 0.20$ to 1.5, Table 2). QL contains the most varied lithic assemblage; metamorphic rock fragments usually dominate the lithic fraction (Lm/Lt > 0.50; Fig. 5d; Table 2), with subordinate volcanic and/or sedimentary rock fragments (Lv + Ls/Lt > 0.25, Table 2). Volcanic rock fragments commonly show propilitic alteration (i.e., to carbonates, epidote, and opaque minerals).

QL petrofacies occurs in two different stratigraphic levels in the lower section of the Paganzo Group: in Namurian-aged glacial diamictites of DI-2 (Cuesta de Huaco and Cerro Guandacol localities; Fig. 6c and d) and in Stephanian-aged coarse-grained sandstones of DI-4 overlying the volcanic rocks in the westernmost portion of the Precordillera (Rincón Blanco locality) (Fig. 6e).

The mixed or recycled orogenic provenance signal that characterizes QL can be interpreted differently for each stratigraphic level (Fig. 6f). In the case of the glacial-related sandstones included in DI-2, mixing of lithologies could have resulted from fluvioglacial activity and resedimentation of plutonic-metamorphic-sourced diamictites with concomitant sedimentary-rich debris incorporation from the Protoprecordillera basement substratum. DI-4 sandstones could be interpreted as the distal expression of the arkosic wedge (QF petrofacies) prograding from the east; the participation of volcanic rock fragments (Fig. 6f) could be explained by volcanism cessation and Protoprecordillera collapse in the westernmost depositional area.

5.5. Quartzolithic-volcanic (QLv) petrofacies

The quartzolithic-volcanic (QLv) petrofacies (Q 69 ± 6 F 14 ± 3 L 17 ± 6, Qm 50 ± 8 F 14 ± 3 Lt 35 ± 11) has a characteristic moderate to high total quartz content, though chert fragments can be locally abundant (Qp/Qm $= 0.2$ to 0.6, Table 2). Mesosilicic and acid volcanic rock fragments clearly dominate the lithic fraction (Lv/Lt $= 0.75$; Fig. 5e), and subordinated sedimentary clasts are more common than metamorphic fragments (Ls/Lm > 1). In addition, K–feldspar grains occur in a greater proportion than plagioclase (Plg/FK < 1) (Table 2).

QLv petrofacies has been identified in DI-4 coarse-grained sandstones at Cuesta de Huaco (Fig. 4). The high amount of quartz and volcanic rock fragments associated with common chert and sedimentary rock fragments suggests that QLv petrofacies resulted from the combined supply of a distal volcanic arc plus some subordinated Protoprecordilleranic basement input (Fig. 6f).

5.6. Volcanolithic-quartzose (LvQ) petrofacies

The volcanolithic-quartzose (LvQ) petrofacies (Q 47 ± 17 F 13 ± 5 L 39 ± 19, Qm 43 ± 16 F 13 ± 5 Lt 43 ± 19) has intermediate to low total quartz content and low polycrystalline quartz (Qp/Qm $= 0.05$ to 0.15). Highly altered basic to mesosilicic volcanic rock fragments clearly dominate the lithic fraction (Lv/Lt $= 0.75$) with subordinate metamorphic rock fragments (Lm/Lt $= 0.18$ to 0.28). Despite the dominant volcanic input, K–feldspar grains (including microcline) remain more common than plagioclase (Plg/FK < 1) (Table 2).

The volcanolithic-quartzose (LvQ) petrofacies is present at Cerro Guandacol as coarse-grained sandstones and sandy matrix of conglomerates that form punctuated intercalations within DI-4 and DI-5 (Fig. 4).

Moderately to highly abundant altered volcanic rock fragments, intermediate to low amounts of quartz, and the presence of microcline indicate LvQ petrofacies is the result of the combined supply of the Carboniferous volcanic arc and distal arkosic input from the Pampean–Famatinean basement (Fig. 6f).

5.7. Volcanolithic (Lv) petrofacies

The volcanolithic (Lv) petrofacies (Q 20 ± 4 F 23 ± 12 L 58 ± 13, Qm 18 ± 3 F 23 ± 12 Lt 59 ± 13) has a remarkably high lithic content, with abundant fresh volcanic rock fragments (Lv/Lt near 1; Table 2, Fig. 5f). Volcanic rock fragments comprise common mesosilicic rocks (andesite to traquite) and minor quantities of riolites and dacites; vitric fragments (tuffs and ignimbrites) are abundant, but

basalt rock fragments rarely occur. Lv is the only petrofacies in which plagioclase clearly dominates over K–feldspar (Plg/FK $\gg$ 1), total quartz is a subordinate component (Q $<$ 20%), and chert fragments can be abundant (Qp/Qm = 0–0.2) (Table 2).

Lv petrofacies is restricted to the westernmost domain of the basin (Rincón Blanco, Fig. 4). Important volcanic activity along the boundary between the Paganzo and Río Blanco basins promoted volcanolithic sandstones to intercalate with andesites and dacites in depositional intervals 1, 2, and 3 (Fig. 4). Field relationships and the compositional affinity of sandstones to their associated volcanic rocks indicate that Lv resulted from syndepositional magmatic activity related to subduction along the paleo-Pacific margin of Gondwana (Remesal et al., 2004).

6. Petrosomes

The term petrosomes was employed by Ingersoll and Cavazza (1991) to describe "consanguineous, regionally correlatable units" that result in three-dimensional rock bodies of genetically related petrofacies, thus pointing to common source areas. The concept of petrosomes would be adequate in the case of lithologically heterogeneous basements, and it is particularly useful to apply in the case of the Paganzo Basin due to the lithological complexity that characterizes its source areas.

Each morphotectonic element envisaged as a source area for the Upper Carboniferous sediments of the Paganzo Basin is represented herein by a petrosome (Table 3). Petrosomes are thus defined by a particular association of petrofacies after provenance interpretations (Fig. 6). Three petrosomes are recognized in the lower section of the Paganzo Group: basement, recycled orogen, and volcanic arc (Table 3).

6.1. Basement petrosome

The basement petrosome includes two petrofacies (QF and QF-Lm) that reflect the continental block provenance of the plutonic-metamorphic basement of the Sierras Pampeanas and Sierra de Famatina systems (Fig. 1). This petrosome constitutes most of the sedimentary fill of the Paganzo Basin and dominates the eastern portion of the depositional area; to the west, the basement petrosome forms an arkosic wedge that diachronically prograded onto the Protoprecordillera (Fig. 4).

6.2. Recycled orogen petrosome

The recycled orogen petrosome combines two petrofacies (QF-Ls and QL) carrying provenance signals from mixed and recycled orogenic provenance areas (Fig. 6). This petrosome has a restricted time and space extent and is only identified in the central portion of the basin (Fig. 4). The presence of a recycled orogen petrosome indicates that the Protoprecordillera acted as a positive element and active source of sediment during Namurian times. The declining participation of this petrosome toward the Carboniferous–Permian boundary suggests that the Protoprecordillera was losing its topographic expression before its final collapse (Limarino et al., 2003).

6.3. Volcanic arc petrosome

The volcanic arc petrosome is represented by three petrofacies (QLv, LvQ, and Lv) that show input from the Carboniferous volcanic arc developed during Wesphalian and Stephanian times along the western margin of the Precordillera (Fig. 6). This petrosome occurs as a very thick stratigraphic interval at the westernmost border of the Paganzo Basin (Rincón Blanco; Fig. 4). An analysis of petrographic parameters in the Lv-QLv-LvQ trend (Table 2) reveals a progressive decrease in the abundance of volcanic rock fragments with a concomitant increase in the amount of monocrystalline quartz grains and the K–feldspar-to-plagioclase ratio. Spatial distribution of this trend highlights localities in paleogeographic positions close to the volcanic center (e.g., Rincón Blanco, Fig. 1) and the progressive loss of the volcanic arc signal due to non-volcanic-sourced sediment incorporation in localities farther east (e.g., Cuesta de Huaco, Cerro Guandacol; Fig. 1).

7. Evolutive model

The model we propose for the evolution of the Upper Carboniferous sedimentary fill of the Paganzo Basin reveals complex spatial and temporal relationships among the petrosomes; this model is intended to honor paleocurrent data and provenance information obtained from sandstones (Fig. 7).

At the beginning of the sedimentary filling of the basin, the recycled orogen petrosome formed a narrow belt close to the Protoprecordillera in the western Paganzo Basin (Fig. 7a). A major episode of sediment recycling and mixing resulted from the glacial and associated postglacial flooding events during the Namurian (Fig. 7b). The recycled orogen petrosome was then progressively covered by, or intertongued with, the basement petrosome prograding from the eastern-sourced, plutonic-metamorphic Sierras Pampeanas and Sierra de Famatina systems (Fig. 7c and d). It is worth noting that in the eastern Paganzo Basin, where the sedimentary pile rests directly on the plutonic-metamorphic basement, the basement petrosome dominates the entire analyzed interval as a very thick arkosic wedge (Figs. 4 and 7d).

Meanwhile, the existence of an important volcanic center located in the westernmost border of the basin during Late Carboniferous times is evidenced not only by volcanic rocks (andesites and dacites) but also by a volcanic arc petrosome (Fig. 7a–c). Thus, the volcanic arc petrosome allows the detection of volcanic activity in central positions of the basin where no volcanic rocks occur (e.g., Cuesta de Huaco, Cerro Guandacol, Fig. 4). The progressive decrease

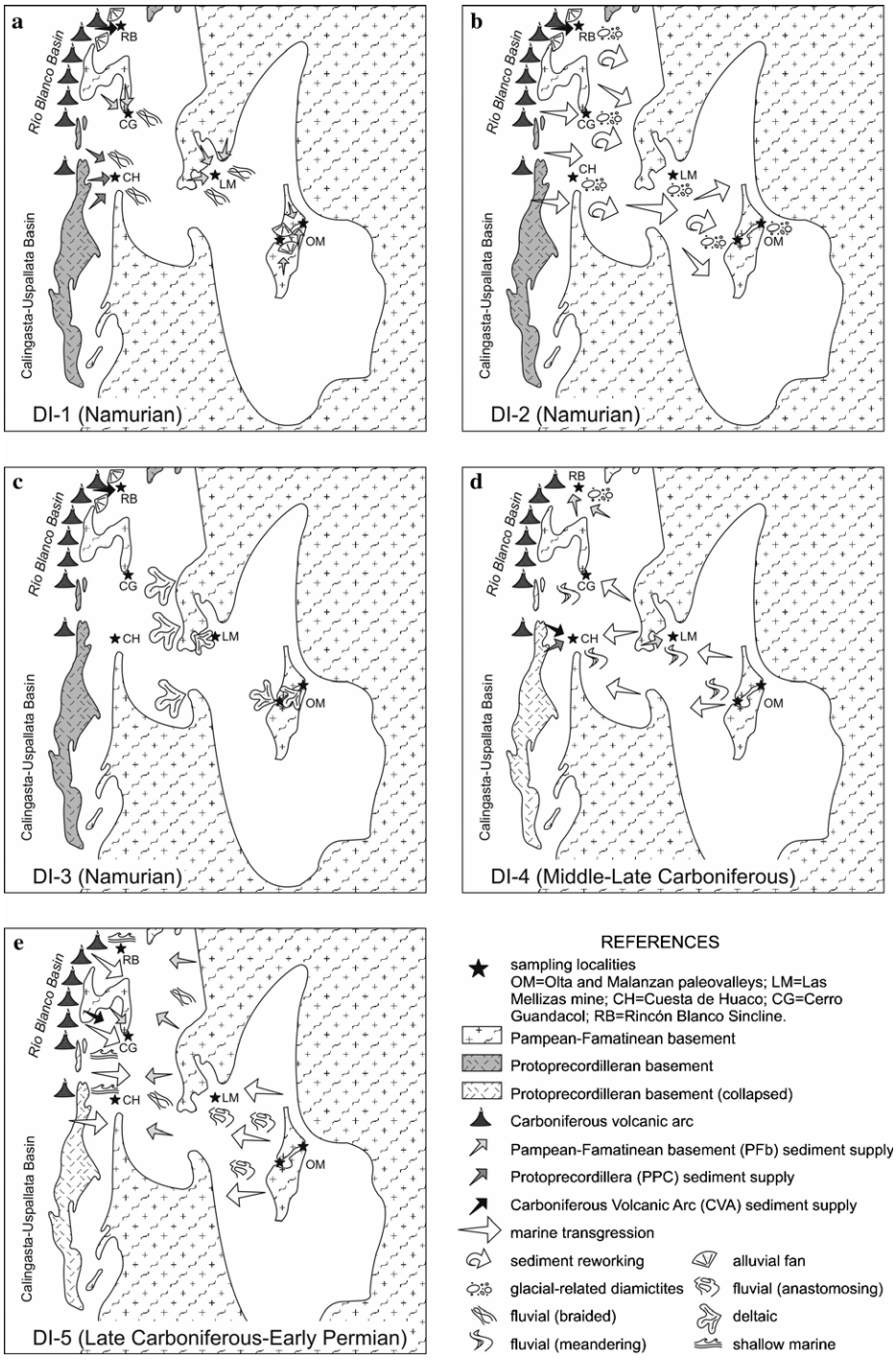

Fig. 7. Proposed evolutive model for sedimentary fill of the Paganzo Basin during the Late Carboniferous–Early Permian. Paleogeography based on interpreted maximum areal extent of the basin, following Salfity and Gorustovich (1983).

in volcanic rock fragment content registered in sandstones of the volcanic arc petrosome from west to east (i.e., Lv to LvQ and QLv petrofacies; see Table 3) suggests dilution of the volcanic arc provenance signature caused by reworking and mixture with nonvolcanic lithologies during sediment transport away from the volcanic chain. The volcanic arc petrosome is diachronically covered by the basement petrosome prograding from the east (Fig. 4). The sharp boundary between the volcanic arc and basement petrosomes at Rincón Blanco constitutes a conspicuous stratigraphic and petrologic discordance (Scalabrini Ortiz, 1973; Net, 1999).

Finally, a second transgressive event during Late Carboniferous–Early Permian times is registered in the western Paganzo Basin (Figs. 3, 4, 7e). By this time, the basement petrosome dominated the whole basin, and only sporadic

participation of volcanic arc-derived sediments has been registered (e.g., LvQ petrofacies in Cerro Guandacol; Table 3). Although this transgression did not reach the eastern portion of the Paganzo Basin, some changes in the style of the fluvial systems in inland positions were interpreted as resulting from this base-level rise.

8. Conclusions

Petrofacies and petrosomes are useful tools to understand the temporal and spatial evolution of the Carboniferous sedimentation in the Paganzo Basin. Whereas petrofacies describe lithological characteristics of source areas in terms of sandstone detrital modes, petrosomes are used herein as assemblages of petrofacies to describe the lithological complexity of the Paganzo Basin substratum adequately.

Three source areas recognized in the Paganzo Basin (Pampean–Famatinean basement, Precordilleranic basement, and Carboniferous volcanic arc) are characterized by seven petrofacies and grouped according to their provenance discrimination in three petrosomes: basement, recycled orogen, and volcanic arc petrosomes.

The Pampean–Famatinean basement is represented by the basement petrosome, which consists of the quartzofeldespathic (QF) and the quartzofeldespathic-metamorphic enriched (QF-Lm) petrofacies. QF derives from granitoids and high-grade metamorphic rocks of the Sierras Pampeanas and Sierra de Famatina systems. QF-Lm represents local low-grade metamorphic and sedimentary rocks of Vendian? – Cambrian age associated with this basement. The plutonic-metamorphic basement constitutes most of the Paganzo Basin substratum, the dominant source area for Upper Carboniferous sediments in the eastern and central domains of the basin. This basement petrosome progrades diachronically from east to west as a clastic wedge of arkosic composition.

The Precordilleranic basement is represented by the recycled orogen petrosome, characterized by the quartzofeldespathic-sedimentary enriched (QF-Ls) and mixed quartzolithic (QL) petrofacies. QLs petrofacies evidences a supply from Early Paleozoic sedimentary rocks (marine limestones, fine-grained siliciclastics) that formed the core of the Protoprecordillera. The mixed provenance signal of the QL petrofacies indicates different interpretations linked to different paleogeographic and paleotectonic frameworks; it can be attributed to the reworking of plutonic-metamorphic-derived sediments on a Protoprecordillera-derived substratum during glacial and postglacial activity (e.g., DI-2 diamictites in western Paganzo Basin) or to the incorporation of volcanic arc-derived material into the distal arkosic wedge after volcanism cessation and Protoprecordillera collapse (e.g., DI-4 sandstones in the westernmost boundary of the basin). This petrosome constitutes evidence of the Protoprecordillera orogenic belt acting as a positive element in the western Paganzo Basin. The geometry of this petrosome and its loss near the Carboniferous–Permian boundary supports the idea of a progressive decrease in relief and final collapse of the Protoprecordillera.

The Carboniferous volcanic arc source area is represented by the volcanic arc petrosome and clearly evidenced by the volcanolithic (Lv), volcanolithic-quartzose (LvQ), and quartzolithic-volcanic (QLv) petrofacies. These three petrofacies register a progressive decrease in the abundance of volcanic rock fragments and a parallel increase in the amount of quartz and the K–feldspar-to-plagioclase ratio, which point to progressively farther paleogeographic positions with respect to the position of the volcanic arc. The volcanic arc petrosome pinches out into sandstones belonging to the basement petrosome without reaching the eastern domain of the Paganzo Basin.

An evolutive model of the sedimentary fill of the Paganzo Basin during Late Carboniferous times is proposed herein. This model is intended to honor observed variations in sandstone composition in time and space registered within the upper section of the Paganzo Group, as well as available paleocurrent and paleoenvironmental data.

Acknowledgments

L.I.N. thanks C.O.L. for supervising her Ph.D. dissertation at the University of Buenos Aires, from which this work resulted. Useful comments on a previous version were provided by Earle F. McBride (University of Texas at Austin). Alfonsina Tripaldi, Mariana Gagliardo, and Martín Santisteban assisted L.I.N. in the field. The Department of Geological Sciences of the University of Buenos Aires provided workplace and general logistics, and special thanks go to the Petrography Research Group for sharing their automated point counter. Financial support was granted by the Agencia Nacional de Promoción Científica y Tecnológica (PICT 04821) and CONICET. The authors are also grateful to *JSAES* referees Walther L. Lecaros and Daniel Poiré for their comments and suggestions that helped improve this manuscript. This work is a contribution to IGCP Project 471.

References

Aceñolaza, F.G., 1971. Geología estratigráfica de la zona comprendida entre Punta de Agua y Rincón Blanco, Dpto. Gral. Lamadrid, La Rioja. Acta Geológica Lilloana XI 7, 125–150.

Andreis, R.R., Spalletti, L.A., Mazoni, M.M., 1975. Estudio geológico del Subgrupo, Sierra de Maz, provincial de La Rioja, República Argentina. Revista de la Asociación Geológica Argentina 30, 247–273.

Andreis, R.R., Leguizamón, R., Archangelsky, S., 1986. El paleovalle de Malanzán: nuevos criterios para la estratigrafía del Neopaleozoico de la Sierra de Los Llanos, La Rioja, República Argentina. Boletín de la Academia Nacional de Ciencias 57 (1/2), 3–119, Córdoba..

Archangelsky, S., González, C., Cúneo, R., Sabattini, N., Césari, S., Aceñolaza, F., García, G., Buatois, L., Ottone, E., Mazzoni, M., Hünicken, M., Gutiérrez, P., 1996. Paleontología, bioestratigrafía y paleoecología de las Cuencas Paganzo, Calingasta–Uspallata, Río Blanco y San Rafael. In: Archangelsky, S. (Ed.), El Sistema Pérmico en

la Argentina y en la República Oriental del Uruguay. Academia Nacional de Ciencias, Córdoba, pp. 177–202.

Azcuy, C.L., Morelli, J.R., 1970a. The Paganzo Basin. Tectonic and Sedimentary Characteristics of the Gondwana Sequences in Northwest Argentina. II Gondwana Symposium pp. 241–247.

Azcuy, C.L., Morelli, J.R., 1970b. Geología de la comarca Paganzo-Amaná, el Grupo Paganzo. Formacionaes que lo componen y sus relaciones. Revista de la Asociación Geológica Argentina 25, 405–429.

Basu, A., 1986. Influence of climate and relief on composition of sand released at source areas. In: Zuffa, G.G., (Ed.), Provenance of arenites, NATO Advanced Study Series 148, 1–18.

Bodenbender, G., 1896. Devono y Gondwana en la República Argentina. Las formaciones sedimentarias de la parte noroeste. Boletín de la Academia Nacional de Ciencias, Córdoba 15, 201–252.

Buatois, L., Limarino, C.O., 2003. El contacto entre las formaciones Hoyada Verde y Tres Saltos, Carbonífero de la Cuenca Calingasta–Uspallata: su reinterpretación como una superficie de incisión de valle fluvial. III Simposio Argentino del Paleozoico Superior, Resúmenes 16, La Plata, Argentina.

Césari, S.N., Gutiérrez, P.R., 2000. Palynostratigraphy of Upper Paleozoic sequences in Central-Western Argentina. Palynology 24, 113–146.

Cisterna, G.A., Sabattini, N., 1998. Algunos Gastropoda de la Formación Río del Peñón (Carbonífero Superior-Pérmico Inferior), provincia de La Rioja, Argentina. Revista de la Asociación Geológica Argentina 53, 212–218.

Cisterna, G.A., Simanauskas, T., 2000. Brachiopods from the Río del Peñón Formation, Río Blanco Basin, Upper Paleozoic of Argentina. Revista Española de Paleontología 15 (2), 129–151.

Critelli, S., Ingersoll, R.V., 1995. Interpretation of neovolcanic versus paleovolcanic sand grains: an example from Miocene deep marine sandstones of the Topanga Group (Southern California). Sedimentology 42, 783–804.

Dickinson, W.R., 1970. Interpreting detrital modes of graywacke and arkose. Journal of Sedimentary Petrology 40, 695–707.

Dickinson, W.R., Rich, E.I., 1972. Petrologic intervals and petrofacies in the Great Valley Sequence, Sacramento Valley, California. Geological Society of America Bulletin 83, 3007–3024.

Dickinson, W., Beard, L., Brakenridge, G., Erjavec, J., Ferguson, R., Inman, K., Knepp, R., Lindberg, A., Ryberg, P., 1983. Provenance of North American Phanerozoic sandstones in relation to tectonic setting. Geologic Society of America Bulletin, 222–235.

Di Paola, E., 1972. Caracterización litoestratigráfica de la Formación Lagares (Carbónico), en Paganzo-Amaná, provincia de La Rioja, República Argentina. Revista de la Asociación Geológica Argentina 27, 99–116.

Fauqué, L., Limarino, C., 1990. El Carbonífero de Agua de Carlos (Precordillera de La Rioja), su importancia tectónica y paleoambiental. Revista de la Asociación Geológica Argentina 46, 103–114.

Fauqué, L., Limarino, C.O., Cingolani, C., Varela, R., 1999. Los movimientos intracarboníferos en la Precordillera riojana. XIV Congreso Geológico Argentino, Actas I, 421–424, Salta..

Fernández Seveso, F., Tankard, A.J., 1995. Tectonics and stratigraphy of the Late Paleozoic Paganzo Basinof western Argentina and its regional implications. In: Tankard, A.J., Suárez, R., Welsink, H.J. (Eds.), Petroleum Basins of South America. American Association Petroleum Geologists, Memoir, pp. 285–301, vol. 62.

Fernández Seveso, F., Pérez, M.A., Brisson, I., Álvarez, L., 1993. Sequence stratigraphy and tectonic análisis of the Paganzo Basin, Western Argentina. XII International Congress Carboniferous Permian Stratigraphy C. Rendues 2, 223–260.

González, C.R., Bossi, G., 1987. Descubrimiento del Carbonífero inferior marino al oeste de Jagüe, La Rioja. IV Congreso Latinoamericano de Paleontología, Actas 2, 713–724.

González Bonorino, G., 1991. Late Paleozoic orogeny in the northwestern Gondwana continent margin, western Argentina and Chile. Journal of South American Earth Sciences 4, 131–144.

Grantham, J.H., Velbel, M.A., 1988. The influence of climate and topography on rock-fragment abundance in modern fluvial sand of the Southern Blue Ridge Mountains. North Carolina. Journal of Sedimentary Petrology 58, 219–227.

Gutiérrez, P.R., Limarino, C.O., 2001. Palinología de la Formación Malanzán (Carbonífero Superior), La Rioja, Argentina: nuevos datos y consideraciones paleoambientales. Ameghiniana 38 (1), 99–118.

Gutiérrez, P.R., Limarino, C.O., 2003. Formación Río del Peñón (La Rioja, Argentina): el perfil del sinclinal del Rincón Blanco y el límite Carbonífero-Pérmico. 12 Simposio Argentino de Paleobotánica y Palinología, Resúmenes 34.

Ingersoll, R.V., 1983. Petrofacies and provenance of Late Mesozoic Forearc Basin, Northern and Central California. American Association of Petroleum Geologists Bulletin 67, 1125–1142.

Ingersoll, R., Cavazza, W., 1991. Reconstruction of Oligo-Miocene volcaniclastic dispersal patterns in north-central New Mexico using sandstone petrofacies. SEPM Special Publication 45, 227–236.

Ingersoll, R.V., Kretchmer, A.G., Valles, P.K., 1993. The effect of sampling scale on actualistic sandstone petrofacies. Sedimentology 40, 937–953.

Johnsson, M.J., 1993. The system controlling the composition of clastic sediments. In: Johnsson, M.J., Basu, A. (Eds.), Processes Controlling the Composition of Clastic Sediments. Geological Society of America, Special Paper 284, pp. 1–19.

Limarino, C.O., 1987. Paleoambientes sedimentarios y paleogeografía de la sección inferior del Grupo Paganzo en el Sistema del Famatina. Anales de la Academia de Ciencias Exactas Físicas y Naturales 39, 149–178.

Limarino, C.O., Gutiérrez, P.R., 1990. Diamictites in the Agua Colorada Formation. New evidence of Carboniferous glaciation in South America. Journal of South American Earth Sciences 3, 9–20.

Limarino, C.O., Sessarego, H., Césari, S.N., López Gamundi, O., 1986. El perfil de la Cuesta de Huaco, estratotipo de referencia (hipoestratotipo) del Grupo Paganzo en la Precordillera Central. Anales de la Academia Nacional de Ciencias Exactas, Físicas y Naturales (Buenos Aires, Argentina) 38, 81–109.

Limarino, C.O., Césari, S.N., López Gamundí, O.R., 1988. Superficies de discontinuidad en el registro sedimentario del Paleozoico Superior de las Cuencas Pacíficas de Argentina. V Congreso Geológico Chileno Tomo II, 37–50.

Limarino, C.O., Césari, S.N., Net, L.I., Marenssi, S.A., Gutierrez, P.R., Tripaldi, A., 2002. The Upper Carboniferous postglacial transgression in the Paganzo and Río Blanco Basins (northwestern Argentina): facies and stratigraphic significance. Journal of South American Earth Sciences 15, 445–460.

Limarino, C., Tripaldi, A., Marenssi, S., Fauqué, L., 2003. Tectonic, sea level and climatic controls on Carboniferous sedimentation in the western basins from Argentina, III Latinoamerican Congress of Sedimentology. Extended abstracts, 295–296, Belem (Brazil)..

Limarino, C.O., Tripaldi, A., Marenssi, S.A., Fauqué, L., 2006. Tectonic, sea-level and climatic controls on Upper Paleozoic sedimentation in the Western basins of Argentina. Journal of South American Earth Sciences (this volume).

LópezGamundí, O.R., Alvarez, L., Andreis, R.R., Bossi, G.E., Espejo, I., FernándezSeveso, F., Legarreta, L., Kokogian, D., Limarino, C.O., Sessarego, H., 1989. Cuencas Intermontanas. In: Chebli, G., Spalletti, L.A., (Eds.), Cuencas Sedimentarias Argentinas, pp. 123–167.

López Gamundí, O., Espejo, I., Conaghan, P., Powell, C., 1994. Southern South America. In: Veevers, J., Powell, C. (Eds.), Permian-Triassic Pangean Basins and Foldbelts along the Panthalassan Margin of Gondwanaland. Geological Society of America, Memoir, pp. 281–329, vol. 184.

Mack, G.H., 1984. Exceptions to the relationship between plate tectonics and sandstone composition. Journal of Sedimentary Petrology 54, 212–220.

Mansfield, C.F., 1971. Stratigraphic variation in sandstone petrology of the Great Valley sequence in the Southern Coast Ranges west of Coalinga, California. GSA Abstracts with Programs (Cordilleran section) 3 (2), 157.

Marenssi, S.A., Tripaldi, A., Caselli, A., Limarino, C.O., 2002. Hallazgo de tillitas sobre el flanco occidental del anticlinal de Agua Hedionda (Provincia de San Juan): evidencias de avances y retrocesos del hielo durante la glaciación gondwánica en la Cuenca Paganzo. Revista de la Asociación Geológica Argentina 57 (3), 349–352.

Morelli, J., Limarino, C.O., Césari, S.N., Azcuy, C., 1984. Caracteríticas litoestratigráficas y paleontológicas de la Formación Lagares en los alrededores de la mina Margarita, provincia de La Rioja. IX Congreso Geológico Argentino, Actas 4, 337–347, San Carlos de Bariloche.

Net, L.I., 1999. Petrografía, diagénesis y procedencia de areniscas de la sección inferior del Grupo Paganzo (Carbonífero) en la cuenca homónima. Ph.D. Thesis, Universidad de Buenos Aires, Buenos Aires, Argentina.

Net, L.I., 2002. Control de la composición de la fracción clástica sobre el tipo de cemento en areniscas carboníferas de la Cuenca Paganzo, Argentina. AAS Revista 9, 1–30.

Net, L.I., Limarino, C.O., 1999. Paleogeografía y correlación estratigráfica del Paleozoico Superior de la Sierra de Los Llanos, provincia de La Rioja, Argentina. Revista de la Asociación Geológica Argentina 54, 229–239.

Net, L.I., Limarino, C.O., 2000. Caracterización y origen de la porosidad en areniscas de la sección inferior del Grupo Paganzo (Carbonífero superior), Cuenca Paganzo, Argentina. AAS Revista 7, 47–70.

Net, L.I., Alonso, M., Limarino, C.O., 2002. Source rock and environmental control on clay mineral associations, Lower Section of Paganzo Group (Carboniferous), Northwest Argentina. Sedimentary Geology 152, 183–199.

Pazos, P.J., 2002. The Late Carboniferous glacial to postglacial transition; facies and sequence stratigraphy, western Paganzo Basin, Argentina. Gondwana Research 5 (2), 467–487.

Ramos, V., 1988. Tectonics of the Late Proterozoic–Early Paleozoic: a collisional history of Southern South America. Episodes 11, 168–174.

Ramos, V.A., Jordan, T.E., Allmendinger, R.W., Mpodozis, C., Kay, S.M., Cortés, J.M., Palma, M.A., 1986. Paleozoic terranes of the Central Argentine–Chilean Andes. Tectonics 5, 855–880.

Remesal, M., Fauqué, L.A., Limarino, C.O., 2004. Volcanismo calcoalcalino neopaleozoico en la Precordillera de La Rioja. Petrología y caracterización litoestratigráfica de la Formación Punta del Agua (Carbonífero Superior-Pérmico Inferior), Precordillera de La Rioja. Revista de la Asociación Geológica Argentina 59 (3), 462–476.

Sabattini, N., Ottone, E.G., Azcuy, C.L., 1991. La zona de Lissochonetes jachalensis-Streptohynchus inaequiomatus (ex Fauna intermedia) en la localidad de La Delfina, provincial de San Juan. Ameghiniana 27, 75–81.

Salfity, J.A., Gorustovich, S.A., 1983. Paleogeografía de la cuenca del Grupo Paganzo (Paleozoico Superior). Revista de la Asociación Geológica Argentina 38, 437–453.

Scalabrini Ortiz, J., 1973. El Carbónico en el sector septentrional de la Precordillera sanjuanina. Revista de la Asociación Geológica Argentina 27 (4), 351–377.

Scasso, R.A., Limarino, C.O., 1997. Petrología y diagénesis de rocas clásticas. Asociación Argentina de Sedimentología, Publicación Especial 1, La Plata, Argentina.

Spalletti, L.A., 1968. Estructuras sedimentarias de la Formación Guandacol (Carbónico). Extremo sur de la Sierra de Maz, provincia de La Rioja. Revista del Museo de La Plata (nueva serie) Sección Geología 6, 235–272.

Sterren, A.F., Martínez, M., 1996. El paleovalle de Olta (Carbonífero): paleoambientes y paleogeografía. XIII Congreso Geológico Argentino y III Congreso de Exploración de Hidrocarburos, Actas II, 89–103, Buenos Aires, Argentina.

Zuffa, G.G., 1980. Hybrid arenites: their composition and classification. Journal of Sedimentary Petrology 50, 21–29.

Zuffa, G., 1985. Optical analysis of arenites: influence of methodology on compositional results. In: Zuffa, G.G., (Ed.), Provenance of arenites. NATO Advanced Study Series 148 165-189.